

## AN EFFECTIVE METHOD TO FIND GREEN'S FUNCTIONS FOR LAYERED MEDIA

N. S. Markov<sup>1\*</sup>, A. M. Linkov<sup>1,2,3</sup>

<sup>1</sup>Peter the Great St. Petersburg Polytechnic University, Russia

<sup>2</sup>Rzeszow University of Technology, Poland

<sup>3</sup>Institute for Problems in Mechanical Engineering of the Russian Academy of Sciences, Russia

\*e-mail: markovnicholas@gmail.com

**Abstract.** Layered structure of rocks strongly influences propagation of hydraulic fractures widely used in practice to increase oil and gas production. The paper aims to facilitate modeling of hydraulic fractures. We develop a method to overcome the main difficulty, which arises when modeling fractures in layered systems: the need in building Green's functions for systems of layers. The method employs highly efficient fast Fourier transform (FFT) in frames of the difference equations method. Its key computational parameters are established by studying bench-mark problems. Green's functions with log-type singularity are included into the theory and the algorithm developed. The accuracy of the method and its application are illustrated with numerical examples.

**Keywords:** layered structures; Green's function; hydraulic fractures; Fourier transform; boundary element method.

### 1. Introduction

Solving problems for systems of layers, containing internal cracks, cavities, pores, inclusions and/or interacting grains, is important for various applications of continuum mechanics, including hydraulic fractures, mining, geomechanics, nano-technology, etc. To account for the internal structure of a layer, the boundary element methods (BEM) is a good choice when fundamental solutions entering appropriate boundary integral equations (BIE) are known or calculated in advance. However, except for the simplest cases of homogeneous infinite space or bonded half-spaces, finding the fundamental solutions (Green's functions) is quite involved and time expensive. It may be notably simplified if the geometry of a problem suggests using methods *ad hoc*. Specifically, simplifications become possible when the layers have parallel plane or spherical (circular in 2D) boundaries. These cases, being of practical significance, we focus on building Green's functions for them. For certainty, the case of layers with plane parallel boundaries is considered. In particular, it is of prime interest for modeling hydraulic fractures.

The specific geometry of layers suggests using the Fourier expansions/transforms. Starting from early sixties of the last century [4,5,22,23], this approach to solving problems for multi-layered media has been employed in numerous papers (e.g. [1,2,6,10–21,26–29]). However, to the date the advantage of using the fast Fourier transform (FFT) has not been employed except for a few papers concerning with particular problems [1,13,14]. The case of Green's functions with log-type singularity, which tend to infinity with growing distance from a source point, has even stayed out of the general scheme sketched in [11].

The *objective* of the present paper is to make a step in developing universal algorithms employing the fast Fourier transform (FFT) for the problems for layered structures. The log-type singular solutions are to be included into the general scheme. For the beginning, we develop such an algorithm and extend the theory to log-type singularities for *plane harmonic problems*. The efficiency of the method suggested is illustrated by examples.

## 2. Problem formulation

For certainty, we discuss the problem formulation in terms used in the elasticity theory. Consider a package of  $n$  elastic layers with plane parallel boundaries (Fig. 1).

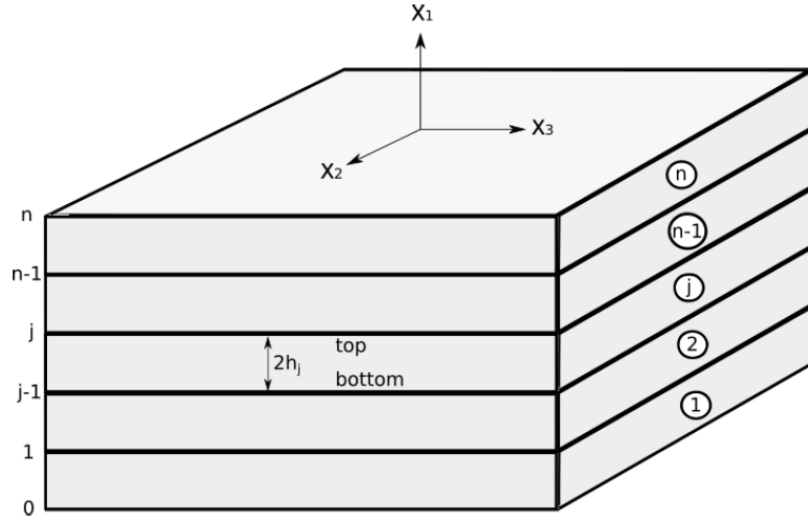


**Fig. 1.** Scheme of a layered structure.

The layers may contain cracks, cavities, pores, inclusions, interacting grains, etc. We numerate the layers from 1 to  $n$  and boundaries from 0 to  $n$ . The superscript “ $i$ ” will denote that a quantity refers to the  $i$ -th layer or to the  $i$ -th contact. The axes  $x_2$  and  $x_3$  are directed along the boundaries in the horizontal plane. The unit normal to layer boundaries is directed along the axis  $x_1$ . Values, corresponding to the top and bottom boundaries of the  $i$ -th layer, are marked with a subscript “ $t$ ” and “ $b$ ”, respectively. Then the displacement discontinuity vector is  $\Delta u^i = u_t^i - u_b^{i+1}$ .

For a system of  $n$  layers, the partial differential equations (PDF) are:

$$L^i u = 0 \quad (i = 1, \dots, n), \quad (1)$$

where  $L^i$  is a differential operator with physical constants of the  $i$ -th layer. Specifically, for elasticity problems, it is the Lamé operator; for harmonic problems, it is the Laplace operator.

The contact conditions at interfaces may include continuity of tractions  $q$

$$q_t^i = q_b^{i+1} = q^i \quad (i = 1, \dots, n - 1) \quad (2)$$

and linear dependence of the displacement discontinuity  $\Delta u$  on the traction

$$-\Delta u^i = A_c^i q^i, \quad (3)$$

where  $A_c^i$  is a square matrix of contact interaction on the boundary between layers  $i$  and  $i + 1$ . If a contact is ideal, then  $A_c^i = 0$  and  $\Delta u^i = 0$ .

On the boundaries of cracks and cavities, the boundary conditions are assigned as

$$-\Delta u = B_c q + \Delta u^0, \quad (4)$$

where  $B_c$  is a symmetric matrix and  $\Delta u^0$  is a prescribed displacement discontinuity. The inversion of (4)  $q = -B_c^{-1} \Delta u + q^0$  with  $q^0 = -B_c^{-1} \Delta u^0$  includes the case when a traction  $q^0$  is assigned. The particular case of assigned tractions corresponds to  $B_c^{-1} = 0$ ; then

$$q = q^0 \quad (5)$$

The problem consists of finding the solution to (1) under the contact conditions (2) and (3) and the boundary conditions (4) or (5).

### 3. Green's function

By using the theory of potential, the problem is reduced to a boundary integral equation (e.g. [3, 7, 8]). It includes the Green's functions. For a layered system, the latter are unknown and to be found by solving the equation:

$$L^i U(x, y) = -\delta(x - y)I \tag{6}$$

for homogeneous (without cracks, cavities, etc.) layers under the contact conditions (2), (3). In (6),  $I$  is the unit matrix;  $\delta(x)$  is the Dirac delta function. The Green's function may be found by following the line of the paper [11]. It is as follows.

Let the singular point  $x$  on the right hand side of (6) is a point  $x^k$  of the  $k$ -th layer in the layered system (Fig. 2a). Consider an infinite homogeneous media with elastic properties of the considered layer. The Green's function for such a medium is the known fundamental solution  $U^0(x, y)$ , say Kelvin's solution of the elasticity theory. The  $l$ -th column of  $U^0$  provides the displacements  $u_t^k$  and tractions  $q^k$  on the top boundary of the  $k$ -th layer, and the displacements  $u_b^k$  and tractions  $q^{k-1}$  on its bottom boundary.

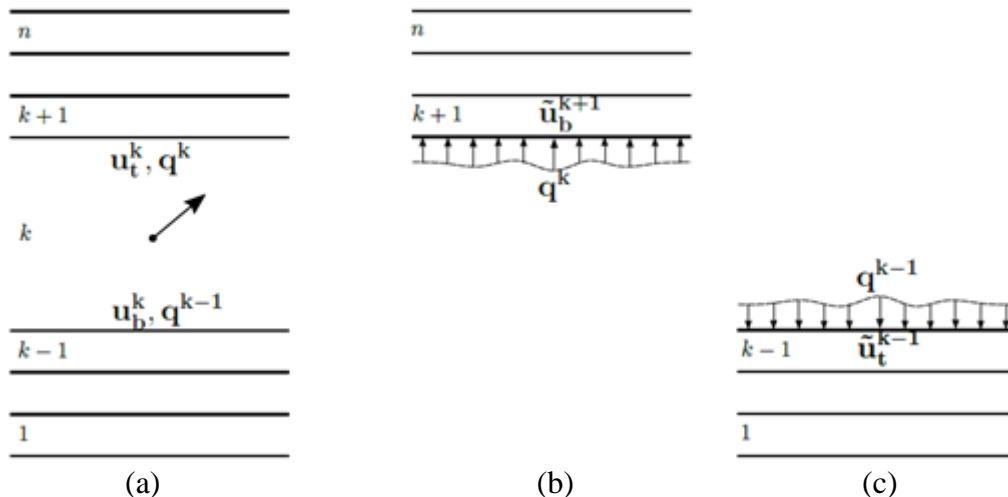


Fig. 2. Schemes to find the Green's matrix.

The needed Green's function  $U(x, y)$  is represented as the sum:

$$U = U^0 + U^a, \tag{7}$$

where  $U^a(x, y)$  is an additional matrix serving to meet the contact conditions (2), (3). This matrix is non-singular in all the layers including the layer  $k$ . It is found by considering separately the upper package of layers (Fig. 2b) and lower package of layers (Fig. 2c) under the loads  $q^k$  and  $q^{k-1}$ , respectively. Hence, the condition (2) of continuity of the tractions is met.

After solving the elasticity problems for these packages, we obtain the displacements  $u^*$  in the upper and lower packages. In particular, the displacements  $u_b^{*k+1}$  on the bottom boundary of the layer  $k + 1$  and  $u_t^{*k-1}$  on the top boundary of the layer  $k - 1$  are known. However, in general, the differences  $u_t^k - u_b^{*k+1}$  and  $u_t^{*k-1} - u_b^k$  do not satisfy the contact conditions (3) on the top and bottom boundaries of the  $k$ -th layer. There appear known discrepancies in the conditions (3), which are to be removed. It is done by solving the problem for the whole system (Fig. 2a) with the prescribed discontinuities (equal to the assigned discrepancies taken with the minus sign) on the top and bottom boundaries of the  $k$ -th layer and with contact conditions (3) on remaining contacts. The correcting solution  $\tilde{u}$  is easily found by the sweep method. Finally, the additional matrix is

$$U^a = U^* + \tilde{U} \quad (8)$$

Then the whole Green's matrix  $U$  becomes the sum of three matrices

$$U = U^0 + U^* + \tilde{U}, \quad (9)$$

of which  $U^0 = 0$  outside the  $k$ -th layer and  $U^* = 0$  inside this layer. In general, the matrix  $\tilde{U}$  is non-zero in all the layers. Thus, to find the Green's matrix we have to solve three similar standard problems. It can be efficiently done by using the Fourier transform and the sweep-method [11].

#### 4. Plane harmonic problem with using FFT

For a plane harmonic problem, the potential  $u$  in each layer satisfies the Laplace equation:

$$\Delta u = \frac{\partial^2 u}{\partial x_1^2} + \frac{\partial^2 u}{\partial x_2^2} = 0 \quad (10)$$

The corresponding vector of the flux  $q$  is

$$q = k \nabla u \quad (11)$$

Herein,  $k$  is the conductivity, taken with the minus sign, in problems of heat (current, fluid) flow;  $k = E/[2(1 + \nu)]$  in anti-plane elasticity problems with  $E$  being the Young's modulus,  $\nu$  the Poisson's ratio.

Instead of the Fourier transform on an infinite interval, we consider a finite interval  $[-A, A]$ . Its length  $2A$  should be sufficiently large to replace an infinite layer with a periodical system having the period  $2A$ . Clearly, the period  $2A$  should notably exceed the thickness of a layer, containing the source point, and also the characteristic size of the structural elements, say cavities, within the layer. Below we shall establish quantitative estimations of  $2A$ , which may be used when building the Green's functions.

It is of essence to perform direct and inverse transforms as efficient as possible. This suggests using the *fast Fourier transform* (FFT) [13,14]. Then the number  $N$  of sampling points is a degree of 2:  $N = 2^m$  where  $m$  is non-zero positive integer. The sampling points  $x_j$  are uniformly distributed on the interval  $[-A, A]$ . For a function  $f(x)$  with values  $f_j = f(x_j)$  at the sampling points  $x_j$  ( $j = -N/2, \dots, N/2 - 1$ ), the direct transform, marked with wave, gives its image  $\tilde{f}_k = \tilde{f}(s_k)$  at  $N$  points  $s_k$  uniformly distributed on the interval  $[-A, A]$  of the axis  $s$ . For certainty, the direct FFT is defined as

$$\tilde{f}_k = \frac{1}{N} \sum_{j=-N/2}^{j=N/2-1} f_j \exp(-2\pi i k j / N) \quad (12)$$

Then the transform inverse to (12) is:

$$f_j = \sum_{k=-N/2}^{k=N/2-1} \tilde{f}_k \exp\left(\frac{2\pi i k j}{N}\right), \quad (13)$$

where  $i = \sqrt{-1}$ . From now on, to keep track with results for layered systems, commonly presented in terms of the Fourier transform on the infinite interval or in terms of Fourier series, we shall employ the usual notation of original functions and their images. We shall write a discrete function  $f_j$  as  $f(x)$  and its discrete image  $\tilde{f}_k$  as  $\tilde{f}(s)$ .

With these agreements, application of the FFT (12) to (10) along the  $x_2$ -axis yields:

$$\Delta \tilde{u} = \frac{\partial^2 \tilde{u}}{\partial x_1^2} - s^2 \tilde{u} = 0 \quad (14)$$

The image  $\tilde{q}^i$  of the component  $q_1$  of the flux  $q$  in the  $i$ -th layer is:

$$\tilde{q}^i = \kappa_i \frac{\partial \tilde{u}}{\partial x_1} \quad (i = 1, \dots, n) \quad (15)$$

By using (14), the contact conditions (2)-(4) are re-written in terms of images. Finally, a harmonic problem for  $n$  homogeneous layers is reduced to the algebraic system of difference equations in fluxes  $\tilde{q}^i$  on the boundaries of layers (see, e.g. [10, 11]):

$$A^i \tilde{q}^{i-1} - C^i \tilde{q}^i + B^i \tilde{q}^{i+1} + F^i = 0, \quad (16)$$

where  $A^i = -R_{tb}^i$ ;  $C^i = -A_c + R_{tt}^i - R_{bb}^{i+1}$ ;  $B^i = R_{bt}^{i+1}$ ;  $F^i = -\Delta \tilde{u}_0^i$  are the images of assigned discontinuities of the potential. For the harmonic problems considered, the coefficients are scalar; the explicit formulae for them are:

$$\begin{aligned} R_{tt} &= \frac{1}{2}(R_s + R_a) \\ R_{tb} &= -\frac{1}{2}(R_s - R_a) \quad R_s = \frac{2}{\kappa s} \coth(sx_1) \\ R_{bt} &= \frac{1}{2}(R_s - R_a) \quad R_a = \frac{2}{\kappa s} \tanh(sx_1) \\ R_{bb} &= -\frac{1}{2}(R_s + R_a) \end{aligned} \tag{17}$$

The images of the potential on boundaries of layers are obtained by employing the dependences used when deriving (16):

$$\begin{aligned} \tilde{u}_t &= R_{tt}\tilde{q}_t + R_{tb}\tilde{q}_b \\ \tilde{u}_b &= R_{bt}\tilde{q}_t + R_{bb}\tilde{q}_b \end{aligned} \tag{18}$$

The solution to the system (16) under assigned boundary conditions on external boundaries of a package, is promptly found by the highly efficient sweep method for any fixed frequency (wave number)  $s$  (see, e.g. [9,25]). Then the images of the solutions to the three standard problems, presented in the previous section, become known. Consequently, the image of the Green's function becomes known, as well. Its inversion through (13) provides the needed Green's function in the physical space.

Alternatively, a system analogous to (16) may be written in terms of the images of the potential on upper boundaries of layers by employing the dependences (18).

### 5. Choice of the period for building log-type Green's function by FFT

In contrast with 3D problems, the starting fundamental solution for 2D elliptic problems has log-type singularity. In particular, in 2D harmonic problems, the Green's function for a homogeneous plane is:

$$U^0 = -\frac{1}{2\pi} \ln(r), \tag{19}$$

where  $r$  is the distance to the point source. It is clear that  $U^0$  tends to infinity with growing  $r$ . However, when applying the Fourier method at a finite interval of a length  $2A$ , a function is assumed periodic with the period  $2A$ . The fundamental solution for the periodic harmonic potential is:

$$U_{per}^0 = -Re \frac{1}{2\pi} \ln \left( \sin \left( \frac{\pi}{2A} z \right) \right), \tag{20}$$

where  $z = x_2 + ix_1$  is the complex coordinate in the system with the origin at the source point.

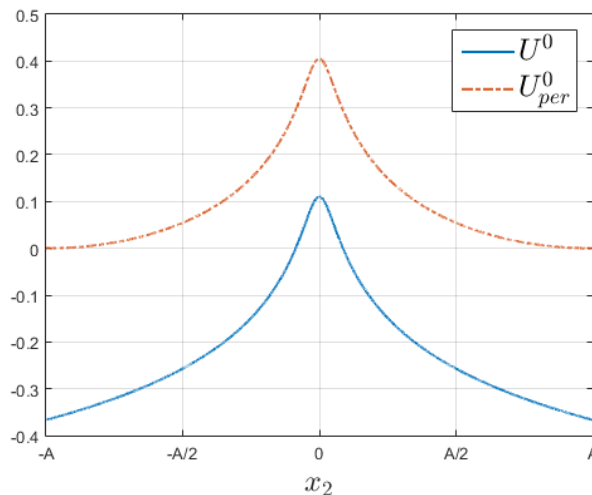


Fig. 3. Graphs of the Green's functions along the  $x_2$ -axis for  $\eta = 20, x_1 = d$ .

The question arises: which period  $2A$  suffices using the Green's function (19) for an infinite plane instead of the Green's function (20) for a periodic (with the period  $2A$ ) problem? Clearly the answer depends on the characteristic size  $2d$  of an area where the Green's function is of interest for a problem considered. Introduce the parameter:

$$\eta = \frac{A}{d} \quad (21)$$

Take into account that the potentials are actually defined to arbitrary constants. This can be seen in Fig. 3, presenting the functions  $U^0$  and  $U_{per}^0$  along the  $x_2$ -axis for  $\eta = 20$ ,  $x_1 = d$ . To exclude the constants, when comparing  $U^0$  with  $U_{per}^0$ , we use the measure  $\zeta$ , defined as the ratio

$$\zeta = \frac{\max_D |C(x_1, x_2)| - \min_D |C(x_1, x_2)|}{\max_D |C(x_1, x_2)|} \cdot 100\%, \quad (22)$$

where  $C(x_1, x_2) = U^0 - U_{per}^0$ ;  $D$  is a square region with the center at the source point and the side  $2d$ . If  $C(x_1, x_2) = const$  in some region, then  $\zeta = 0$  in this region. The dependence of  $\zeta$  on the ratio  $\eta = A/d$  is presented in Fig. 4.

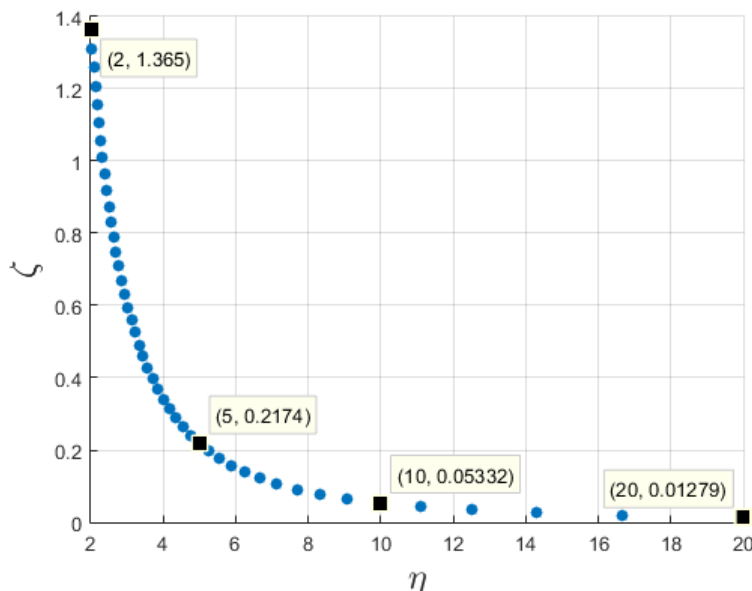


**Fig. 4.** Dependence of the ratio  $\zeta$  on the relative period  $\eta$ .

It can be seen that  $\zeta$  tends to zero when  $\eta$  grows. This confirms that with growing interval of periodicity, its ends exert rapidly decreasing influence on a region with sizes of order  $d$  under consideration. To the accuracy of 0.053 percent, the value of  $\eta$  may be set 10 when using the function  $U^0$  instead of  $U_{per}^0$ .

## 6. Choice of the number of sampling points

There are three plane harmonic problems, for which the Green's functions of log-type have simple analytical forms. They serve us as benchmarks to properly choose the number of sampling points when employing the FFT to find Green's functions for a layered medium. The first problem is that for a *homogeneous* medium with the Green's function given by (19). The second is the problem for a half-plane with *zero flux* at its boundary. It serves to estimate influence of low-permeable (highly compliant in elasticity problems) layers above or/and below a layer with much greater permeability (rigidity). The third problem is for a half-plane with *zero potential* at its boundary. It corresponds to the opposite limiting case and serves to estimate influence of highly-permeable (highly rigid in elasticity problems) layers above or/and below a layer with much less permeability (rigidity).

The two limiting problems provide the thresholds of the accuracy of numerical finding the Green's functions in a region of size  $2d$  for various numbers  $N$  of sampling points located on various intervals  $2A$  of periodicity. The first problem, being intermediate, gives typical accuracy, when neighbors of a layer, containing the source point, have conductivity (rigidity), which does not drastically differs from that of the layer. The tests 1, 2 and 3 below refer, respectively, to the first, second and third problems.

**Test 1.** Consider two homogeneous half-planes with a package of  $n$  homogeneous layers between them. The point source acts in the  $i$ -th layer. All layers have the same conductivity and ideal contacts at interfaces. Such a structure is actually a homogeneous isotropic plane. The Green's function for it is given by (19).

As above, distinguish the region of interest as a square  $D$  with the center at the source point and the sides  $2d$ . The accuracy is estimated by the maximum relative error in this region:

$$\xi = \max_D \left[ \frac{q_i^a}{q_i^0} \right] \cdot 100\%, \tag{23}$$

where  $q_i^a$  is the flux on the  $i$ -th boundary, corresponding to the additional function  $U^a(x, y)$  in (7);  $q_i^0$  is the flux defined by the exact fundamental solution (19). The errors, found for various numbers  $N$  of the sampling points, are summarized in Table 1 when the relative period  $\eta = A/d$  increases from 8 to 64. The results, presented in Table 1, are obtained for a particular structure consisting of five layers ( $n = 5$ ); they stay the same for any other number of layers.

Table 1. The relative error (in %) in the region  $D$  as a function of  $N$  and  $\eta$  for a homogeneous medium

	$N = 128$	$N = 256$	$N = 512$	$N = 1024$
$\eta = 8$	0.605	0.588	0.58	0.576
$\eta = 16$	0.402	0.388	0.382	0.379
$\eta = 32$	0.143	0.134	0.131	0.129
$\eta = 64$	0.104	0.04	0.038	0.037

From Table 1 it can be seen that the influence of the period on the accuracy is notably greater than the influence of the number of sampling points. Better accuracy for large values of  $\eta$  is due to the fact that with growing period  $2A$ , the influence of its boundaries on the region of interest  $D$  rapidly decreases.

**Test 2.** Consider two half-planes, lower of which has the unit conductivity, while the upper has the conductivity tending to zero. The source point is located in the lower half-plane. We represent each of the half-planes by packages of layers of the same thickness and conductivity and find the additional solution  $U^a$  in (7) by solving the problem for the layered system.

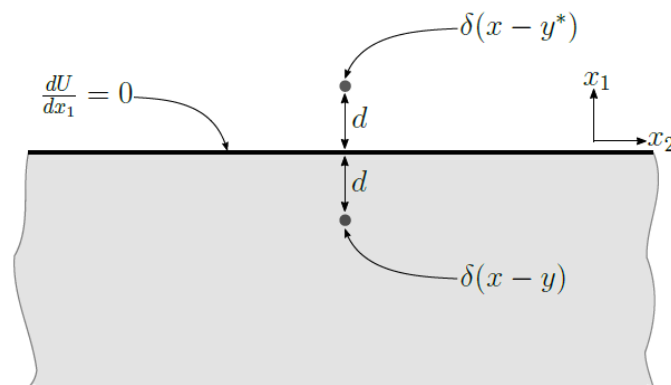


Fig. 5. A point source in a half-space.

For impermeable upper half-plane (Fig. 5), the exact Green's function is the sum of the Green's function (19) for homogenous infinite plane and that of the reflected source, located symmetrically with respect to the boundary and having the same (unit) intensity:

$$U = -\frac{1}{2\pi} \ln(r) - \frac{1}{2\pi} \ln(r^*), \quad (24)$$

where  $r^*$  is the distance from the reflected source.

The Green's function, found as a result of numerical calculations, must have the additional term  $U^a$  close to the term corresponding to the reflected source. As an error, we consider the maximal relative error in the region  $D$ :

$$\xi = \max_D \left[ \frac{q_i^a - q_i^*}{q_i^*} \right] \cdot 100\%, \quad (25)$$

where  $q_i^a$  is the calculated additional flux on the  $i$ -th boundary;  $q_i^*$  is the flux corresponding to the reflected source in (24). The values of  $\xi$  are summarized in Table 2.

Table 2. The relative error (in %) ( $\times 10^{-4}$ ) in the region  $D$  as a function of  $N$  and  $\eta$  for a half-space with impermeable boundary.

	$N = 128$	$N = 256$	$N = 512$	$N = 1024$
$\eta = 8$	2.5755	2.575	2.5748	2.5747
$\eta = 16$	2.5703	2.57	2.5698	2.5697
$\eta = 32$	2.5637	2.5635	2.5633	2.5632
$\eta = 64$	2.562	2.561	2.561	2.5609

The data presented in Table 2 show that the error is practically the same for all the considered pairs  $N$  and  $\eta$ . It remains on the level of  $2.57 \cdot 10^{-4}\%$ . Therefore, the case of low-conductive boundary is quite favorable for the accuracy of the method developed.

**Test 3.** Consider again two half-planes, lower of which has the unit conductivity, while now the upper has the conductivity tending to infinity. In this case, the exact Green's function is obtained by taking the reflected source with opposite sign:

$$U = U^0 + U^* = -\frac{1}{2\pi} \ln(r) + \frac{1}{2\pi} \ln(r^*) \quad (26)$$

We again use equation (25) to estimate errors. The relative errors are summarized in Table 3.

Table 3. The relative error (in%) in the region  $D$  as a function of  $N$  and  $\eta$  for a half-space with a highly conductive boundary.

	$N = 128$	$N = 256$	$N = 512$	$N = 1024$
$\eta = 8$	1.212	1.177	1.16	1.152
$\eta = 16$	0.804	0.777	0.764	0.758
$\eta = 32$	0.286	0.269	0.261	0.257
$\eta = 64$	0.21	0.08	0.076	0.074

From the table it follows that for highly permeable boundary, the error is merely two-fold greater than that for the first problem. In the both cases, to improve the accuracy, it looks preferable to increase the interval of periodicity rather than the number of sampling points.

The comparison of the results in Tables 1, 2 and 3 for the cases 1, 2, and 3, respectively, shows that, as could be expected, the case 1 is intermediate between the two limiting. Still, the results for the case 1 are closer to those for the case 3.



### 7. Application of the method to a harmonic boundary value problem

Consider an example of building and using the harmonic Green's function for a plane layered system. The  $j$ -th layer contains a cavity with the contour  $L_s$  (Fig. 6). The region of interest  $D$  includes the parts by  $D_s$  and  $D^*$ , which are respectively inside and outside the cavity. The contour  $L_s$  is travelled in the direction which leaves the area  $D^*$  to the left; the normal  $n$  is directed to the right to this direction. The superscript plus (minus) refers to the limit from the side with respect to which the normal is outward (inward). The flux  $q_n^0$  is assigned on the counter  $L_s$ . The problem consists of finding the potential  $u$  in the region  $D^*$ .

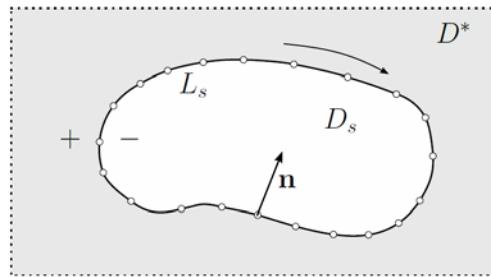


**Fig. 6.** The geometric scheme for a cavity in layered structure.

To find the solution, we need to build the Green's functions  $U_*$  and  $Q_*$  entering the complex boundary integral equations (C-BIE) for plane harmonic problems [8]:

$$Re \left\{ -\frac{1}{2\pi} \int_{L_s} [q_n^+(\tau)U(\tau - z)ds + u^+(\tau)Q(\tau - z)d\tau] \right\} = \begin{cases} ku(z), & z \in D^* \\ \frac{1}{2}\kappa^+u^+, & z \in L_s, \\ 0, & z \notin D^* + L_s \end{cases} \quad (27)$$

where  $\tau, z$  are coordinates in the complex plane;  $q_n^+ = q_n^0$  is the assigned flux. When having  $U$  and  $Q$  the solution to the BIE, given in the second line of (27), is found by the BEM. Having it, the first line of (27) provides the flux within the region  $D^*$ .

We built the Green's functions  $U$  and  $Q$  by the method described in Sec. 3 and 4. Specifically, they are represented as the sums of known Green's functions and additional functions  $U^a(\tau, z)$  and  $Q^a(\tau, z)$ :

$$U = \ln(\tau - z) + U^a(\tau, z); \quad Q = i \frac{\kappa^+}{\tau - z} + Q^a(\tau, z) \quad (28)$$

The parameters of the FFT transform are chosen in accordance with estimates of Sec. 4 and 5. Standard translations along the  $x_2$ -axis are used to adjust the images, obtained for point sources in the local system with the origin at a source point, to the global system used in the BIE (27).

### 8. Example of circular cavity in a layered structure

Assume that there is a circular cavity of the radius  $R \leq h_d$  within the second layer of a three-layered structure. The flux  $q_n^0$  is constant on the boundary of the cavity. The geometrical and physical parameters used for calculations are:

- Half-heights of the layers:  $h_1 = h_3 = 2h_2$
- Conductivities of the layers:  $\kappa_1 = 25\kappa_2, \kappa_3 = 2\kappa_2$
- The period  $2A$  of the interval assumed in FFT:  $2A = 40h_2$
- The number of sampling points of the FFT:  $N = 1024$
- The number of boundary elements on the cavity contour:  $N_s = 90$
- The total intensity of the assigned flux  $\int_{L_s} q_n^0 ds = -1$

The results of calculations of the potential in the layered system with cavities of different radii are presented in Fig.7-10.

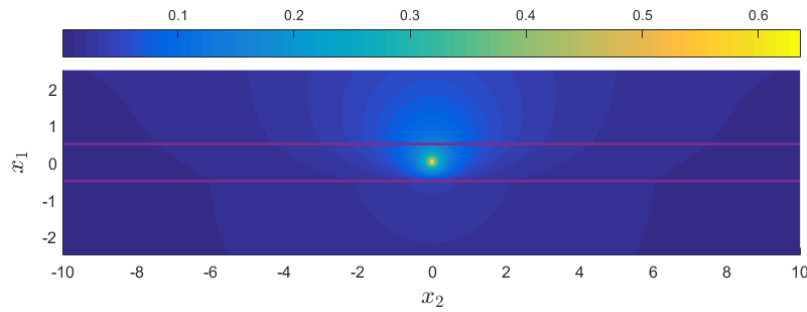


**Fig. 7.** The field of the potential for a circular cavity of radius  $R = 10^{-4}h_2$ .

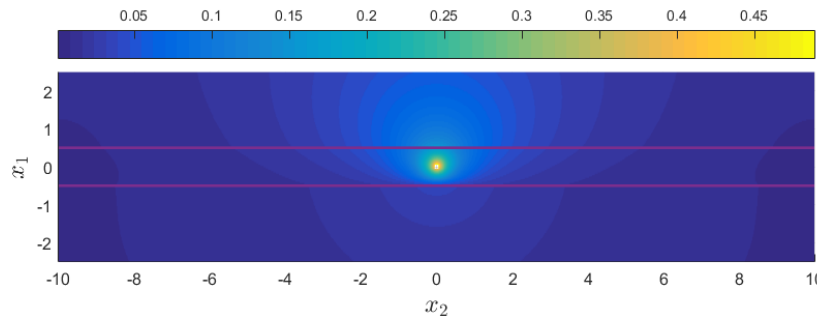


**Fig. 8.** The field of the potential for a circular cavity of radius  $R = 0.1h_2$ .

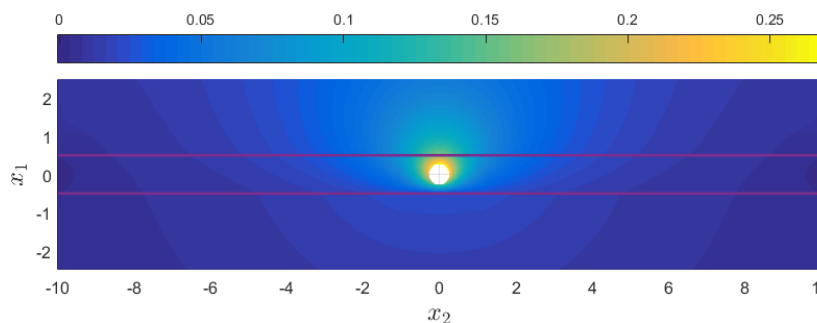


**Fig. 9.** The field of the potential for a circular cavity of radius  $R = 0.5h_2$ .

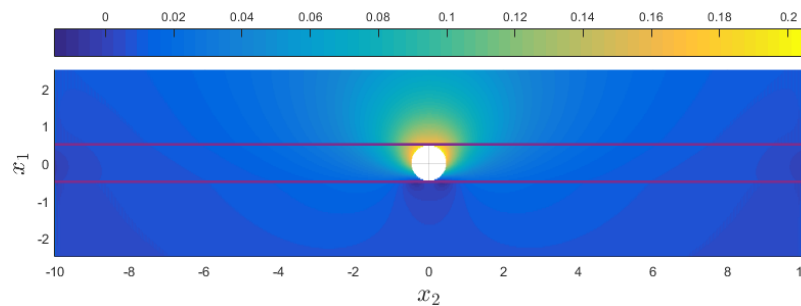


**Fig. 10.** The field of the potential for a circular cavity of radius  $R = 0.9h_2$ .

The results demonstrate that the method developed may serve for efficient solving harmonic and elasticity problems for layers with quite different thicknesses and physical properties.

**Acknowledgement.** This research was financed by Ministry of Education and Science of the Russian Federation within the framework of the Federal Program "Research and development in priority areas for the development of the scientific and technological complex of Russia for 2014-2020", Activity 1.2., Agreement on Grant No. 14.575.21.0146 of 26 September, 2017, unique identifier: RFMEFI57517X0146.

## References

- [1] M. Al Heib, A. M. Linkov, V. V. Zoubkov, In: *International Symposium of the International Society for Rock Mechanics (EUROCK 2001)*, ed. by Sarkka & Floranta (Swets&Zeitinger Lisse, Espoo, 2001), 795.
- [2] F. G. Benitez, L. Lu, A. J. Rosakis // *Int. J. for Numerical Methods in Engineering*, **36** (1993) 3097.
- [3] C.A. Brebbia, J.C.F. Telles, L.C. Wrobel // *Journal of Applied Mathematics and Mechanics*, **65** (1984) 259.
- [4] H. Buffler // *Ingenieur-archiv*, **30** (1961) 417.
- [5] H. Buffler // *Ingenieur-archiv*, **31** (1962) 229.
- [6] H. Buffler // *Journal of Elasticity*, **1** (1971) 125.
- [7] S.L. Crouch, A.M. Starfield, *Boundary Element Method in Solid Mechanics* (Cambridge University Press, Cambridge, 1983).
- [8] A.A. Dobroskok, A.M. Linkov // *Journal of Applied Mathematics and Mechanics*, **73** (2009) 313.
- [9] S.K. Godunov, V.S. Ryabenkii, *Difference Schemes* (North Holland, 1987).
- [10] A.M. Linkov, N.A. Filippov // *Meccanica*, **26** (1991) 195.
- [11] A.M. Linkov, A.A. Linkova, A.A. Savitski // *International Journal of Damage Mechanics*, **3** (1994) 338.
- [12] A.M. Linkov, N.A. Filippov, L.A. Milova, V.V. Zoubkov, In: *Advances in Rock Mechanics*, ed. by Yunmei Lin (USA-World Scientific Publications Co, New York, 1998), 135.
- [13] A.M. Linkov, V.V. Zoubkov, M. Sylla, M. al Heib, *Spectral BEM for multi-layered media with cracks or/and openings*. (IABEM 2000 Symposium, Brescia, Italy) 141.
- [14] A.M. Linkov, V.V. Zoubkov, In: *Proceedings of the XIX International Conference BEM & FEM-2001*, ed. by V.A. Postnov (St. Petersburg, 2001), 236 (in Russian).
- [15] G. Maier, G. Novati, In: *Proceedings of the 7th Intrnat. Conf. on Boundary Elements in Engineering* (Como, 1985), 1.
- [16] G. Maier, G. Novati // *Engineering Analysis*, **3** (1986) 208.
- [17] G. Maier, G. Novati // *International Journal for Numerical and Analytical Methods in Geomechanics*, **11** (1987) 435.
- [18] V.S. Nikishin, G.S. Shapiro, *Problems of Elasticity Theory for Multi-layered Media* (Nauka, Moscow, 1973) (in Russian).
- [19] E.I. Obolashvili, *Fourier Transform and its Application in the Theory of Elasticity* (Tbilici, Metcierba, 1979) (in Russian).
- [20] A.P. Peirce, E. Siebrits // *Comput. Methods Appl. Mech. Engrg.* **190** (2001) 5935.
- [21] A.P. Peirce, E. Siebrits // *International Journal of Fracture*, **110** (2001) 205.
- [22] R.M. Ruppoport // *Proc. Hydrotechnical Institute, Leningrad* (1963) 3 (in Russian).
- [23] R.M. Ruppoport // *Proc. Hydrotechnical Institute, Leningrad* (1966) 149 (in Russian).
- [24] A.A. Samarskii, E.S. Nikolaev, *Numerical Methods for Grid Equations* (Nauka, Moscow, 1978).
- [25] A.A. Samarskii, A.V. Gulin, *Numerical Methods* (Nauka, Moscow, 1989).
- [26] U.A. Shevliakov, *Matrix Algorithms in the Theory of Elasticity for Inhomogeneous Media* (Visha Shcola, Kiev-Odessa, 1977) (in Russian).
- [27]. E. Siebrits, A.P. Peirce // *Int. J. Numer. Meth. Engng.* **53** (2002) 691.
- [28] I.E. Vigdorovich, V.D. Lamziuk, A.K. Privarnikov // *Reports of Ukrainian Acad. Sci., A* (6) (1979) 434 (in Russian).
- [29] L.J. Wardle, *Stress Analysis of Multilayered Anisotropic Elastic Systems Subject to Rectangular Loads* (CSIRO Institute of Earth Resources, Melbourne, 1980).